Vol. 636: 139–156, 2020
https://doi.org/10.3354/meps13226

MARINE ECOLOGY PROGRESS SERIES
Mar Ecol Prog Ser

Published February 20

Horizontal and vertical movement of yellowtails *Seriola quinqueradiata* during summer to early winter recorded by archival tags in the northeastern Japan Sea

Seishiro Furukawa[1,*], Akira Kozuka[2], Toshihiro Tsuji[3], Hiroshi Kubota[1]

[1]Japan Sea National Fisheries Research Institute, Japan Fisheries Research and Education Agency, 1-5939-22, Suido-cho, Chuo, Niigata 951-8121, Japan

[2]Fisheries Research Institute, Toyama Prefectural Agricultural, Forestry and Fisheries Research Center, 364 Takatsuka, Namerikawa, Toyama 936-8536, Japan

[3]Ishikawa Prefecture Fisheries Research Center, 3–7 Ushitsushinko, Noto, Housu, Ishikawa 927-0435, Japan

ABSTRACT: Yellowtails *Seriola quinqueradiata* are an important fishery resource around Japan. Here we investigated the movement ecology and habitat utilization of this migratory fish. Archival tags were implanted in 26 adult yellowtails (61–90 cm in fork length) to examine their seasonal movement patterns and vertical distribution. Yellowtails were captured and released around Noto Peninsula in the Japan Sea on 27 May 2004. Eight individuals were recaptured more than 2 mo later, and we analyzed their daily position and vertical movement with ambient water temperature recorded in 60 or 120 s intervals. Most yellowtail individuals moved from the central coast of Japan to the north (from the west of Tsugaru Strait to the west of Hokkaido) in June. Individuals resided in the northern part of the Japan Sea from summer to mid-fall (late July to late October). Seasonal thermoclines developed during this northward movement and subsequent period of residency, with individuals primarily occupying the surface mixed layer during the daytime and at night; however, individuals made frequent short dives through the thermocline, especially during the daytime. These phenomena may be related to foraging based on the distribution of their prey. In late October, yellowtails started a rapid southward movement, primarily remaining in vertical thermal mixing coastal areas, and not entering the coldwater masses that formed offshore. This southward movement pattern might indicate that yellowtails avoid cold offshore water temperatures.

KEY WORDS: Yellowtail · Archival tag · Movement · Vertical movement · Japan Sea

1. INTRODUCTION

The movement and distribution patterns of many marine fishes are often driven by changing environmental conditions (Crawshaw 1977, Magnuson et al. 1979, Block et al. 2011, Secor 2015, Hays et al. 2016). Understanding the external factors that influence the movement patterns of organisms is essential for establishing a movement ecology paradigm (Nathan et al. 2008). This information is also useful for optimizing fisheries management and marine conservation (McGowan et al. 2017, Lowerre-Barbieri et al. 2019). Yellowtail *Seriola quinqueradiata* is a migratory fish species that is also an important fishery resource around Japan. However, while the fishery for this species is strongly influenced by oceanographic conditions, such as water temperature structure (Hara 1990, Tian et al. 2012), advances in tracking technology and analysis of movement processes have not been used to elucidate the mechanism of this influence in yellowtails.

*Corresponding author: furuks17@affrc.go.jp

The distribution of yellowtails extends from the continental shelf of the East China Sea (ECS) to the coastal waters of Hokkaido, both in the Japan Sea and the Pacific Ocean (Fig. 1). The primary spawning grounds of this species extend from the ECS to the coast off of west Kyushu, Japan. The main spawning season is in the spring and tends to start earlier in the southern reaches of the spawning area (Mitani 1960, Yamamoto et al. 2007, Shiraishi et al. 2011). The larvae of yellowtails that hatch in the main spawning grounds are carried by the surface layer of the Tsushima Warm Current and Kuroshio Current to the waters around Japan (Fig. 1; Ochiai & Tanaka 1986). Juvenile yellowtails are associated with drifting seaweed (Ohno 1984, Uehara et al. 2006, Hasegawa et al. 2017) during spring and early summer (Ochiai & Tanaka 1986). During this period, Japanese fishers locate drifting seaweed mats to collect juvenile yellowtails for use as aquaculture seed stock. When juvenile yellowtails attain a total length of approximately 16 cm, they leave drifting seaweed and recruit to the coastal waters of Japan (Mitani 1960).

The movement characteristics of yellowtails after recruitment to coastal waters have been studied by mark–recapture (Tanaka 1984, Murayama 1992, Yamamoto et al. 2007) and archival tagging (Ino et al. 2008). These studies indicated that juvenile yellowtails (age 0–1) exhibit restricted movement, as most fish were recaptured near the release area. However, adult yellowtails make large-scale movements from Hokkaido to the main spawning ground in the southern part of Japan (Ino et al. 2008). Yellowtails are mainly caught by set nets and purse seines in Japan (Kubota et al. 2019a). The set net fisheries for yellowtails are traditionally important in Japan. For example, large-sized yellowtails caught by set nets in winter are called 'Kan-Buri' (winter-yellowtail); these fish have a high market price and are important as traditional gifts, particularly in the prefectures around Toyama Bay near the middle of the Japan Sea (Fig 1). The fishery conditions that determine yellowtail catch rates with set nets largely depend on the distribution and movement patterns of the fish, which are influenced by oceanographic conditions (Hara 1990, Tian et al. 2012). For example, the water mass structure, such as the location and movement of coldwater eddies formed offshore in the Japan Sea, affects the southward movement pattern and fisheries conditions for yellowtails (Ogawa 1976, Hara 1990).

Electronic tagging has emerged as a powerful tool for elucidating the movement patterns of fish, and

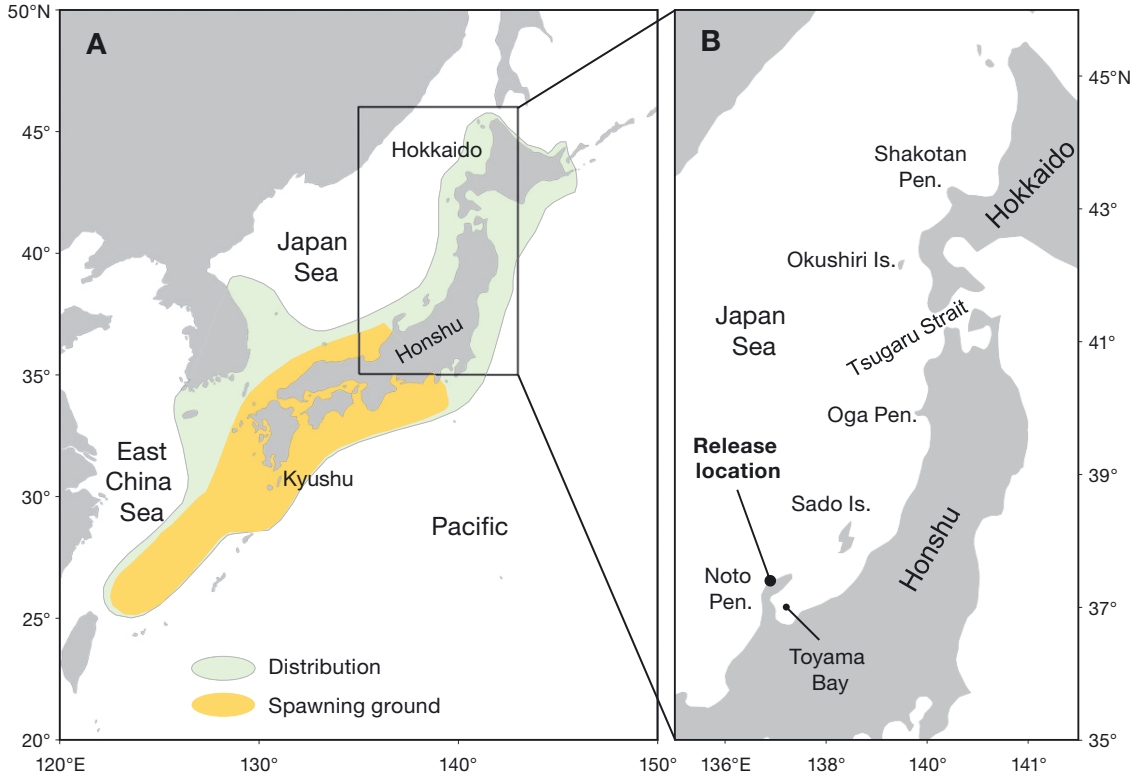

Fig. 1. (A) Distribution and spawning grounds of yellowtails *Seriola quinqueradiata* (adapted from Kubota et al. 2019a) and (B) the study area

how these patterns are correlated with oceanographic conditions (Kitagawa et al. 2004, 2007, Block et al. 2011, Brownscombe et al. 2017, Furukawa et al. 2017, Chmura et al. 2018, Fujioka et al. 2018). This information is used in fisheries management and stock assessments (Taylor et al. 2011, Carvalho et al. 2015, Sippel et al. 2015). A pilot study by Kasai et al. (2000) used electronic temperature–depth recorders to record the spatial and diurnal movement patterns of age-1 juvenile yellowtails in relation to environmental conditions (such as temperature and wind) in Sagami Bay, on the Pacific side of Japan. However, the temperature–depth recorders used in this previous study did not measure fish position; thus, the horizontal movement pattern could only be inferred from ambient environmental conditions.

In comparison, Ino et al. (2008) identified 3 migratory patterns in 26 age-4+ yellowtails in the Japan Sea using archival tags providing light-based geolocation data: (1) migrants between the ESC and west coast of Hokkaido, (2) migrants between the ESC and the Noto Peninsula or Sanin district, and (3) residents that remained around the Noto Peninsula for more than 1 yr. Spawning yellowtails migrated from the Japan Sea to the ECS spawning grounds on the shelf edge zone of the East China Sea and south of Kyushu, Japan (Ino et al. 2008). However, raw geolocations derived from light-based algorithms are often very noisy, and the errors in position estimates can be hundreds of kilometers (Gunn et al. 1994, Musyl et al. 2001, Sibert et al. 2003). A widely used, and in most cases successful, approach to make sense of these raw geolocations is based on a state-space model (Lam et al. 2008, 2010, Jonsen et al. 2013). Unfortunately, however, a study in which archival tagging was applied to yellowtails did not use this state-space approach and only roughly estimated the individual position of one point per month using an ad hoc approach (Ino et al. 2008). Therefore, that study could not examine the behavioral response of yellowtails to spatiotemporal changes in water temperature structure on a fine scale (Ino et al. 2008).

In the present study, we aimed to examine how the migratory pathways and swimming behavior of yellowtails are associated with the spatiotemporal change in temperature structure of the ocean. To accomplish this objective, we used archival tags to collect data on the swimming depth, ambient temperature, and geographic position of free-ranging adult yellowtails in the Japan Sea. We analyzed horizontal and vertical movements of yellowtails in relation to spatiotemporal changes in the temperature structure of the ocean.

2. MATERIALS AND METHODS

2.1. Tags, attachment, and data collection

The main body of the archival tag used for the present study (LAT 2310; Lotek Wireless) was 16.0 mm in diameter, 76 mm long, and weighed 45.0 g. A thin, flexible stalk, 154 mm long, was attached to the main body. The sensors for light and external temperature were embedded at the end of the stalk, while the sensors for pressure and internal temperature were installed in the main body of the tag. Data on external and internal temperature, swimming depth, and light levels were collected every 60 or 120 s. The resolutions of the depth and temperature channels were 0.25 m and 0.02°C, respectively.

On 27 May 2004, yellowtails were captured using set nets near the Noto Peninsula of the Japan Sea (Fig. 1). In this set net, fish could swim after entering the net, and net hauling was usually conducted every day every day. Archival tags were implanted with a sterile scalpel, which was used to make a small (2.0–3.0 cm long) incision through the ventral wall, through which a tag was inserted into the peritoneal cavity. A total of 26 yellowtails, ranging from 61 to 90 cm in fork length, had tags inserted and were released in the vicinity of the set net used to capture them. Of these fish, 17 (65.4% of the total) were recaptured. However, abnormal readings were detected in the temperature and light intensity data of 5 individuals (e.g. continuous recording of water temperatures below −10°C), which were therefore excluded from the analysis. Data for 8 individuals were obtained for 2 or more months; hence, only these 8 individuals were included in the study (Table 1). These fish were considered to be 4+ yr old based on fork length, the age at which they reach maturity (Shiraishi et al. 2011, Kubota et al. 2019a). However, no movements to spawning grounds were observed during the present study period (see Section 3 and Fig. 1), and most of our data acquisition period was outside of the spawning period. Therefore, it was assumed that the present data did not include spawning movement or behavior.

2.2. Geolocation data analysis

The light level data were processed using the template-fit algorithm (Ekstrom 2007) provided by the tag manufacturer (LAT Viewer Studio, Lotek Wireless) to return raw location estimates. We used a Bayesian switching state-space model (SSSM), as described by Jonsen et al. (2005, 2013) and Jonsen (2016), to refine

Table 1. Fork length, period of deployment, recording duration, and summary statistics (means ± SD with maximum values or ranges given in parentheses) for swimming depth and ambient temperature of yellowtails *Seriola quinqueradiata*

Fish ID	Fork length (cm) Release	Recapture	Period of analysis (d)	Swimming depth, m (maximum)	Ambient temperature, °C (range)
A1393	85	94	1-Jun to 9-Dec-2004 (192)	28.9 ± 25.2 (247.0)	19.0 ± 2.4 (2.2–24.4)
B2820	80	91	1-Jun to 28-Nov-2004 (181)	28.0 ± 23.1 (291.5)	20.2 ± 2.0 (4.4–24.6)
B2821	86	94	1-Jun to 26-Nov-2004 (179)	20.3 ± 18.1 (256.0)	19.4 ± 2.0 (4.1–24.5)
B2824	86	93	1-Jun to 9-Dec-2004 (192)	29.8 ± 26.1 (253.9)	19.5 ± 2.1 (2.2–24.7)
B2826	85	92	1-Jun to 9-Dec-2004 (192)	28.8 ± 24.6 (229.5)	19.6 ± 2.1 (2.8–24.1)
B2827	87	93	1-Jun to 10-Dec-2004 (193)	21.4 ± 20.4 (282.5)	18.8 ± 2.2 (3.5–24.1)
B2832	82	92	1-Jun to 13-Dec-2004 (196)	26.6 ± 23.5 (260.2)	19.2 ± 2.1 (2.7–24.7)
B2883	85	90	1-Jun to 20-Dec-2004 (203)	26.1 ± 21.9 (259.2)	19.0 ± 2.1 (4.2–24.7)

the raw geolocation estimates to create the most probable track and to estimate the behavioral state of yellowtails. We modeled the movement of yellowtails as a compound first-difference correlated random walk model, because it is possible to separate this model into 2 or more discrete behavioral states. In brief, the model distinguished 2 movement states: (1) a 'rapid movement' state, which included relatively fast and typically directionally persistent movement, and (2) a 'resident or slow movement' state, which included relatively slow movement that had frequent course reversals (Fig. 2). This model is able to discriminate stochastic switches between behavioral states, with the 2 states being defined by a unique combination of 2 movement parameters: (1) the mean turn angle θ_{b_t} and (2) the persistence of movement b_t, which denotes the behavioral state at time t, where b = 1 (rapid movement) or 2 (resident or slow movement).

This state-space model is composed of a process model and observation model. The process model is described as:

$$\mathbf{x}_t = \mathbf{x}_{t-1} + \gamma_{bt}\,\mathbf{T}(\mathbf{x}_{t-1} - \mathbf{x}_{t-2}) + \text{MultiNormal}(0,\boldsymbol{\Sigma}) \quad (1)$$

where $\mathbf{x}_t$ and $\mathbf{x}_{t-1}$ are the unobserved true locations of fish at times t and t–1. In order to allow for lesser degrees of autocorrelation we add the term γ_{b_t}, with $\gamma_{b_t} = 0$ yielding a random walk and $0 < \gamma_{b_t} < 1$ yielding a random walk with correlation in both direction and moving speed. $\mathbf{T}$ is a matrix describing the mean turn angle, θ_{b_t}, between displacements $\mathbf{x}_t - \mathbf{x}_{t-1}$ and $\mathbf{x}_{t-1} - \mathbf{x}_{t-2}$:

$$\mathbf{T} = \begin{bmatrix} \cos\theta_{b_t} & -\sin\theta_{b_t} \\ \sin\theta_{b_t} & \cos\theta_{b_t} \end{bmatrix} \quad (2)$$

and $\boldsymbol{\Sigma}$ is a variance-covariance matrix specifying the magnitude of stochasticity in 2-dimensional (longitude and latitude) movement:

$$\Sigma = \begin{bmatrix} \sigma^2_{\text{lon}} & \rho\sigma_{\text{lon}}\sigma_{\text{lat}} \\ \rho\sigma_{\text{lon}}\sigma_{\text{lat}} & \sigma^2_{\text{lon}} \end{bmatrix} \quad (3)$$

Switching between behavioral states is regulated by a Markov chain that has fixed transition probabilities:

$$\Pr(b_t = i \mid b_{t-1} = j) = \alpha_{ji} \quad (4)$$

where α_{ji} is the probability of switching from behavioral state j at time t – 1 to behavioral state i at time t. In a 2-state context, α_{ji} represents the elements of a 2 × 2 transition matrix:

$$\boldsymbol{\alpha} = \begin{bmatrix} \alpha_{11} & \alpha_{12} \\ \alpha_{21} & \alpha_{22} \end{bmatrix} = \begin{bmatrix} \alpha_{11} & 1-\alpha_{11} \\ \alpha_{21} & 1-\alpha_{21} \end{bmatrix} \quad (5)$$

where α_{11} and α_{22} are the probabilities of remaining in b = 1 and b = 2, respectively; α_{12} and α_{21} are the probabilities of switching from b = 1 to b = 2 and from b = 2 to b = 1, respectively. These transitions are estimated by assuming a first-order Markov categorical distribution. In practice, it is only necessary to estimate α_{11} and α_{21}, because the rows of α must add up to 1.

Location uncertainty is accounted for via the observation model. We assumed a t-distribution for the error structure of the observation model because its heavy tails allow for large measurement errors. The observation model for this model was specified as:

$$\boldsymbol{y}_t = \mathbf{x}_t + \text{tdist}(0,\beta_c\phi_{t,c},\nu_c) \quad (6)$$

where $\phi_{t,c}$ are the scale parameters for each coordinate c (i.e. latitude and longitude) at time t, which was estimated by the template-fit algorithm (Ekstrom 2007) provided by the tag manufacturer (LAT Viewer Studio, Lotek Wireless); β_c is a correction factor that allows for variability in the scale of error arising from variability among tags; and ν_c represents degrees of freedom for the t-distribution.

Environmental temperature and bathymetry masks were applied to constrain the range of location estimates. Sea surface temperature (SST) is frequently used to improve light-based geolocation from archi-

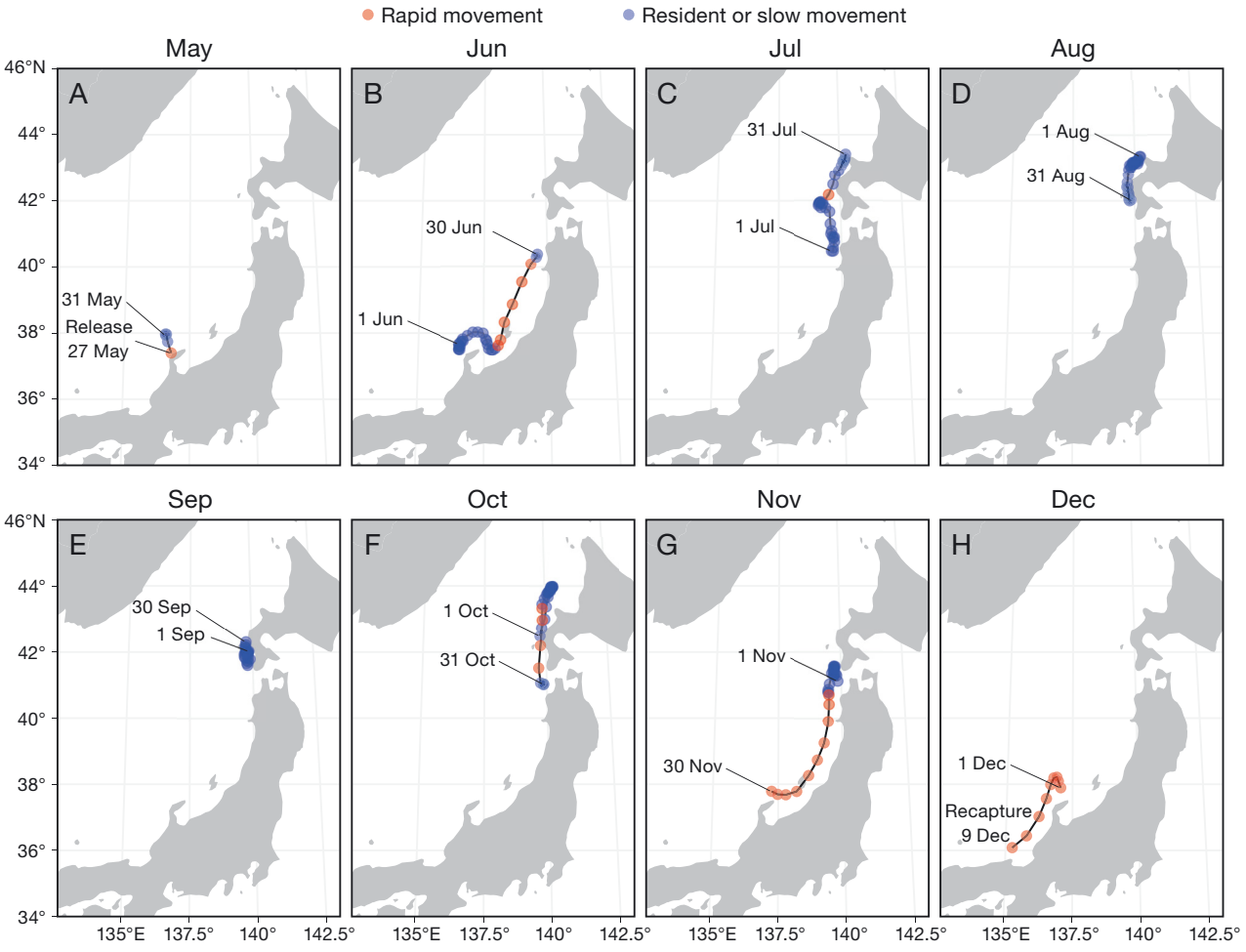

Fig. 2. Monthly change in the locations of an individual archival tagged yellowtail *Seriola quinqueradiata* (tag number B2826) with state estimates from the switching state-space model overlaid in red and blue. Orange circles are state estimates associated with rapid movement; blue circles are state estimates associated with resident or slow movement

val tags (Teo et al. 2004, Nielsen et al. 2006, Lam et al. 2008, 2010). Unfortunately, 16.8–39.1 % (for the 8 individuals) of daily surface temperatures were not recorded because the individuals remained at depths greater than 10 m. The shallowest daily swimming depths for all tagged individuals ranged from 5.3 to 47.7 m, although these fish seemed to be distributed above the thermocline. Therefore, the ambient temperature recorded in the shallowest layer of each 10 m bin recorded by the tags was used and compared to reanalyze model depth–temperature products each day from the 'Four-dimensional Variational Ocean Reanalysis for the western North Pacific' (FORA-WNP30, 0.1° resolution; Usui et al. 2017). We also used the 0.1° resolution bathymetry gridded dataset of the ETOPO1 1 Arc-Minute Global Relief Model (Amante & Eakins 2009) via the 'marmap' package (Pante & Simon-Bouhet 2013) of R 3.6.1 (R Core Team 2019). The constraint was incorporated into the SSSM as:

$$o_t = \text{Bernoulli}(p_t) \tag{7}$$

where o_t is a dummy variable of 1 s (termed the 'Ones Trick' in WinBUGS; Lunn et al. 2000) that is of the same length as the number of location states x_t to be estimated; p_t is the associated probability from a likelihood, which was assumed as:

$$p_t = \begin{cases} 0, & z_t < t_{\text{tag},t} \\ \text{Normal}\left(T_{\text{FORA},t} \mid T_{\text{tag},t}, \sigma^2\right), & z_t \geq t_{\text{tag},t} \end{cases} \tag{8}$$

where z_t is the bathymetric value of the 0.1° grid cell containing location state x_t, and $z_{\text{tag},t}$ is the daily maximum swimming depth. $T_{\text{tag},t}$ is the mean ambient temperature of the shallowest 10 m depth bin containing the daily minimum tag-recorded depth. $T_{\text{FORA},t}$ is the temperature of FORA-WNP30 at the

depth closest to the depth level of FORA-WNP30 at which $T_{tag,t}$ was obtained, and σ^2 is fixed at 0.5. This approach constrained the estimation of location state x_t so that it had zero probability of occurring in water where the bathymetry was shallower than the tag-recorded maximum depth, and a high probability of occurring in water where the ambient temperature of the shallowest layer recorded by the tag matched the temperature of FORA-WNP30.

We used JAGS (Plummer 2017) software from R to fit the SSSM to yellowtail tracks via a Markov chain Monte Carlo (MCMC) analysis in the 'rjags' package (Plummer 2016). We removed geolocations outside the possible range of this species (latitude 20°–50° N, longitude 120°–150° E) before fitting the SSSM; otherwise the model did not converge. In all cases, 2 MCMC chains of 22 000 000 samples were run, and the first 2 000 000 from each chain were discarded as burn-in. Thinning values were set to 1000 to reduce within-chain sample autocorrelation. Although the parameters were estimated as probability distributions, because we performed Bayesian estimations, the plots that were developed of the tracks and the data that were analyzed used the posterior median of the longitude, latitude, and behavioral state estimates.

2.3. Temperature and depth data analysis

To visualize the thermal structure around the tagged fish, a temperature-at-depth matrix with 1 d bins and 10 m depth bins for all individuals was constructed by calculating the mean temperature in each depth bin within each time bin. As a proxy for thermocline depth, we defined the isothermal layer depth (ILD) as the depth at which temperature changed by −0.8°C relative to 10 m depth (Kara et al. 2000). For all days, we calculated the ILD using the temperature data of FORA-WNP30 (0.1° resolution; Usui et al. 2017) at the estimated daily fish location. The frequency distribution of swimming depth during the daytime and nighttime was calculated each month for each 10 m bin. The vertical temperature structure was determined by calculating the mean value for each bin.

Although yellowtails spent most of their time within the surface mixed layer, they sometimes made frequent short-duration dives through the thermocline (see Section 3). A dive was defined as starting when a descending fish passed below the ILD and ending when the fish ascended above the ILD. Dive depth was defined as the greatest depth reached during a dive. Dive duration was the time that elapsed during a single dive. Dives that extended more than 50 m from the ILD (dive depth − ILD > 50 m) were used in the dive analysis.

2.4. Clustering analysis of daily vertical movement patterns

To examine the diving behavior and depth distribution of yellowtails in more detail, we performed a *k*-means cluster analysis. This method has frequently been used to categorize the behavior of diving animals (Schreer & Testa 1996, Lesage et al. 1999, Davis et al. 2003, Sakamoto et al. 2009, Yasuda et al. 2013). To classify daily vertical movement patterns, we aggregated the daily behavioral components (i.e. mean depth, standard division of depth, maximum depth, mean dive depth, mean dive duration, number of dives) for each day and night, which were used in the *k*-means analysis. Whether daytime dive or nighttime dive was determined based on the intermediate time of dive. If a fish did not dive on a given day, then dive depth, dive duration, and the number of dives were set to 0. The *k*-means analysis was performed using pooled data of all individuals. To determine the number of clusters (*k*), we used the gap statistic (Tibshirani et al. 2001), which is one of the most popular and reliable algorithms used to predict the optimum number of clusters. We used the 'fviz_nbclust' function of R 3.6.1 (R Core Team 2019) to determine the number of clusters via the gap statistic. The optimum number of clusters was estimated to be 7 (see Section 3). Details on the gap statistic algorithm are available in Tibshirani et al. (2001).

2.5. Statistical analysis

Generalized additive mixed models (GAMMs) were used to quantify the relationship between oceanographic parameters and the spatial distribution of yellowtails. GAMMs allow for multiple nonlinear relationships between a response variable and its covariates in a semiparametric manner (Wood 2008). To make general inferences about the spatial distribution of tagged yellowtails, we calculated the monthly cumulative total number of observed days for each individual in 0.5° × 0.5° grid cells within the area of the Japan Sea that was south of 50° and east of 134°, and included 0 observations. These values were compared against monthly mean oceanographic parameters (i.e. SST, ILD, chlorophyll *a*) in each grid cell using GAMM. Monthly mean SSTs and ILDs in each grid cell were calculated from the temperature data of FORA-

WNP30. Monthly composite chlorophyll *a* concentrations (9 km resolution, measured by Aqua-MODIS) were downloaded from the Ocean Color Web (https://oceancolor.gsfc.nasa.gov/), and the mean values in each cell were calculated. The longitude and latitude value of the center of the grid cell was also used as a GAMM covariate. A regional effect and soap film spline (Wood et al. 2008) were used to impose land restrictions for this term. Specifically, GAMMs were fitted with a negative binomial distribution, log link function, and random effect of individual yellowtails. Grid cells with an SST of less than 9°C were excluded from the GAMM analysis to reduce calculation time. Because the SST ranged from 13.1 to 23.1°C in each grid cell where tagged yellowtails were detected, it was considered that sufficient results could be obtained even when excluding SST of less than 9°C. Multinomial logistic regression (MLR) with a random effect model was used to quantify how the oceanographic parameters and movement state affected the fraction of the vertical behavioral mode (see Section 3), and was fitted with a multinomial distribution, logit link function, and random effect of individual yellowtails. GAMM and MLR were constructed in R using the 'mgcv' package. Model selection was based on an information-theoretic approach through the minimization of the Bayesian information criterion. Unless stated otherwise, all errors in this paper are reported as 1 SD.

3. RESULTS

3.1. Horizontal movement

One fish (B2826) rapidly moved north in June, resided near the west coast of Hokkaido from August to October, and moved south starting in late October or early November (Fig. 2). This fish occupied an area to the east of the release location and started rapid movement northward on 23 June, reaching the western part of Tsugaru Strait within 6 d (Fig. 2B). Most tagged fish began a northward and rapid movement state in June (Figs. 2B, 3, & 4A,H,O). During this northward movement phase (mostly in June), the mean travel distance in the rapid movement state ranged from 36.4 ± 20.0 km d^{-1} (B2827) to 62.3 ± 33.7 km d^{-1} (B2883), with a maximum value of 96.1 km d^{-1} (B2883) (Fig. 3C). In July, all tagged fish had reached locations near the west coast of the Tsugaru Strait, and were horizontally distributed along the west coast of Hokkaido in August (Figs. 2 & 4). The horizontal movement state showed that these fish resided in this region from July to August (Figs. 2C & 4B,C,I,J,P,Q), and remained in the area to the west of Hokkaido (Figs. 2E,F & 4D,E,K,L,R,S) from September to October.

From late October to early November, all fish started the southward movement along the coast from Hokkaido to Honshu. The frequency of the rapid movement state increased during this period (Fig. 3A), with individual travel distances ranging from 32.9 ± 12.9 to 60.8 ± 27.7 km d^{-1} (range of maximum individual daily distances: 47.1–101.4 km). Some fish reached the area around Noto Peninsula in November to December

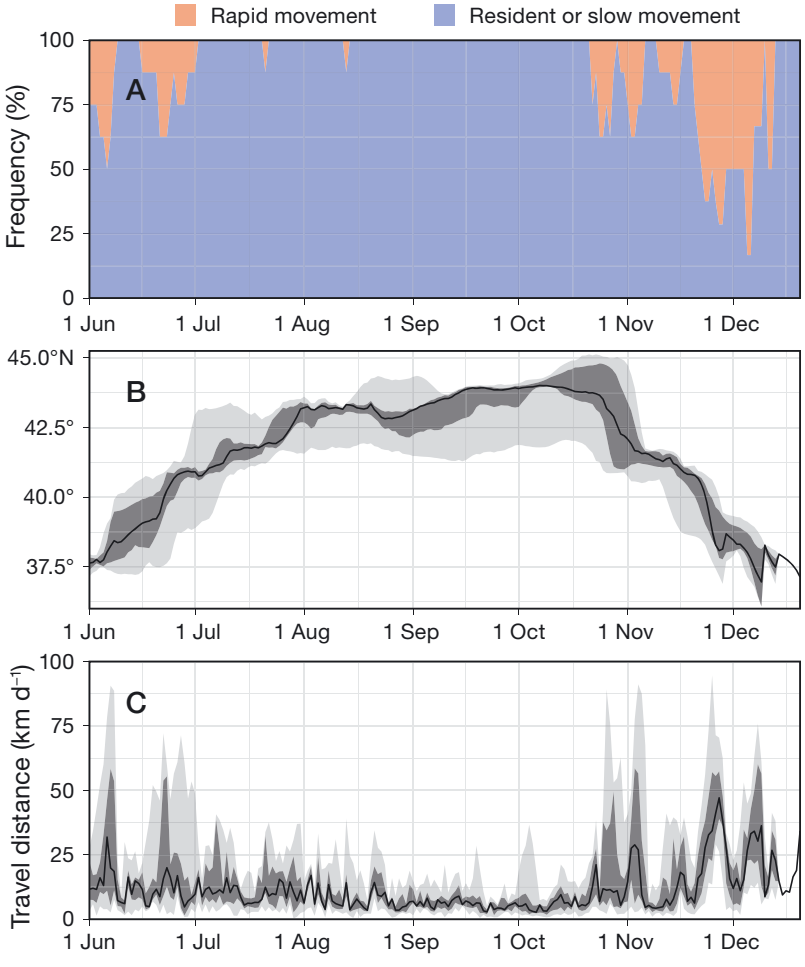

Fig. 3. Daily change in (A) fraction of state estimates from the switching state-space model, (B) latitude, and (C) travel distance per day for all tagged yellowtails *Seriola quinqueradiata*. The medians are represented by solid lines, and dark grey and light grey shaded areas represent the 50th and 95th percentiles, respectively

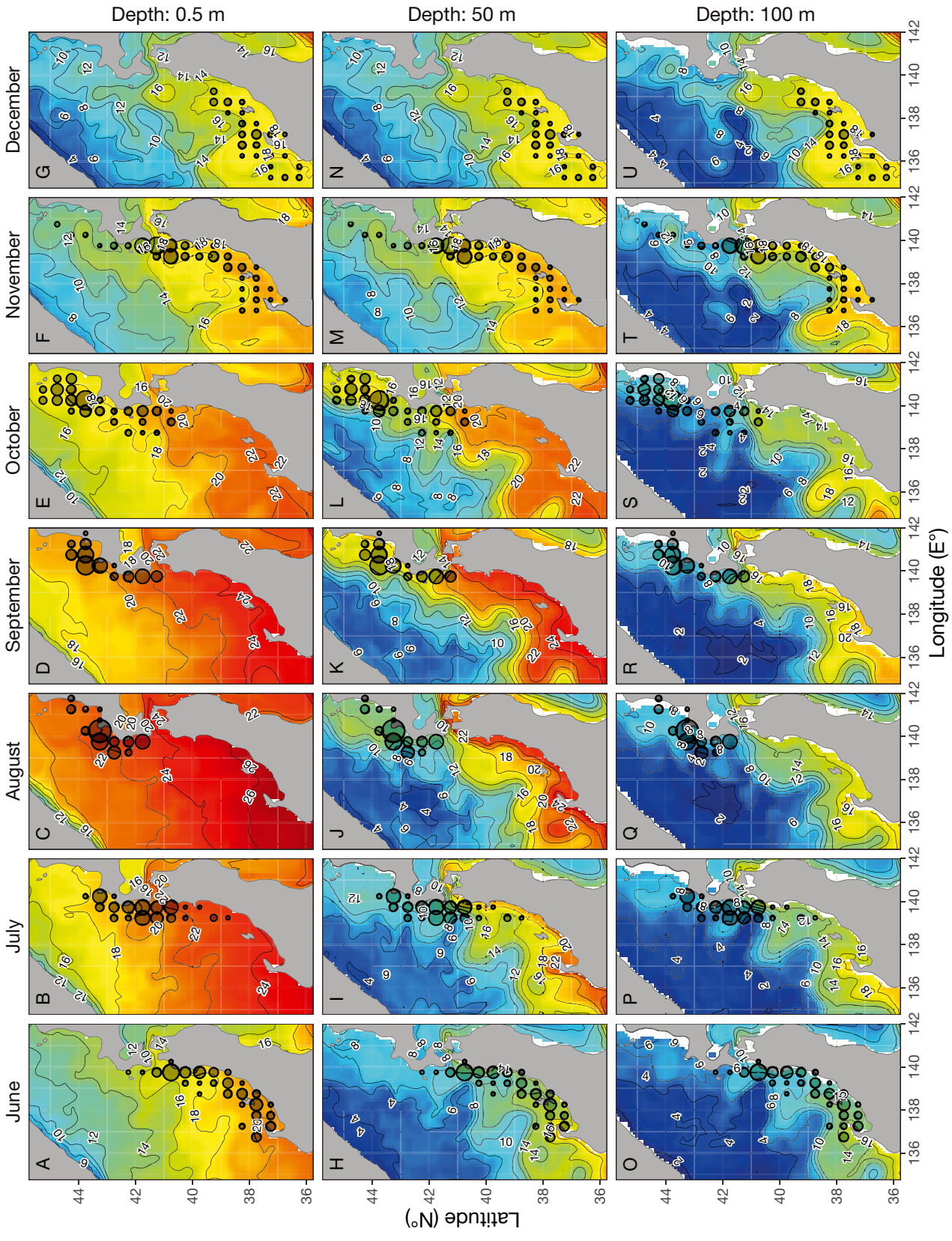

Fig. 4. Monthly change in yellowtail *Seriola quinqueradiata* distribution plotted over subsurface (0.5, 50, 100 m) temperature images. Circle size indicates the cumulative total number of observed days in each 0.5° × 0.5° grid cell, and data are from all individuals pooled

(Fig. 4F,G,M,N,T,U). During this southward movement (November to December), a coldwater mass formed offshore, particularly around the northern part of Sado Island. The coldwater mass edge located near Sado Island in December was characterized by an SST of 14–16°C (Fig. 4G) and ILD of 80–100 m (see Fig. 8N), while the water temperature at 100 m depth was 10–14°C (see Fig. 5U). Yellowtails rarely entered this offshore coldwater mass (Fig. 4F,G, M,N,T,U).

3.2. Vertical movement

A total of 1527 daily vertical movement modes were observed from the 8 fish, and were classified into 7 clusters. For the general visualization of diurnal changes in the vertical distribution and movement of each cluster, we calculated the median, 50th, and 95th percentile values of the depth and diving depth throughout the thermocline at 1 h intervals from 00:00 to 24:00 h local time (Fig. 5). The daily behavioral components for each cluster from all pooled individuals are summarized in Table 2. Cluster 1 was predominant (44.9% of all tracks), and corresponded to the high use of the surface, both during the daytime and nighttime, with occasional shallow dives during the daytime (Fig. 5A,H, Table 2). Mean daytime dive depth, dive duration, and number of dives per day for Cluster 1 were 79.5 ± 10.6 m, 16.9 ± 28.1 min, and 0.0 ± 10.6 (Table 2). We referred to Cluster 1 as the 'surface' behavior mode. Clusters 2, 3, and 4 had common characteristics, with fish swimming in the surface layer at night, with repeated short dives to greater depths, usually during the daytime. Although the number of clusters was determined using gap statistics as an index, Clusters 2, 3, and 4 showed similar vertical movement patterns (Fig. 5B–D, I–K), and it might not be ecologically relevant to separate them into 3 behavior modes. Therefore, these 3 modes were grouped as a single mode termed 'diel brief deep dive' (DBDD) behavior. Cluster 5 was distinguished by constant deep swimming.

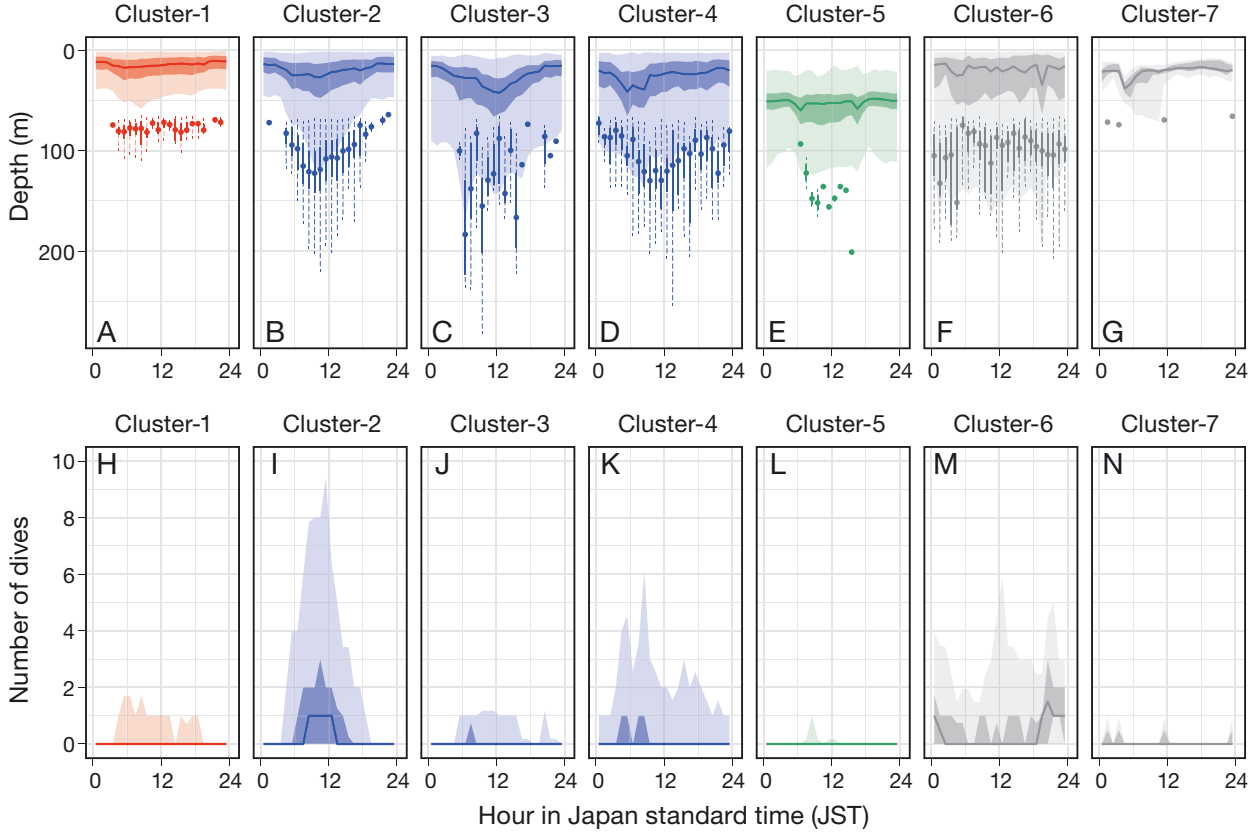

Fig. 5. (A–G) Hourly change in overall swimming depth for the median (solid line), 50th (darker shading), and 95th (lighter shading) percentile, and dive depth across the thermocline for the median (circle), 50th (vertical solid line), and 95th (vertical dashed line) percentile in each cluster. (H–N) Hourly change in number of dives for the median (solid line), 50th (darker shading), and 95th (lighter shading) percentile. Colors indicate behavioral modes (red: surface; blue: diel brief deep dive [DBDD]; green: continuous deep swimming [CDS]; grey: other) and data were pooled from all individuals

Table 2. Frequency and mean ± SD of overall swimming depth, number of dives, dive depth, and dive duration for all behavioral clusters. CDS: continuous deep swimming; DBDD: diel brief deep dive

Cluster	Vertical movement mode	Frequency (%)	Overall swimming depth (m)		Dive frequency (d^{-1})		Dive depth (m)		Dive duration (min)	
			Day	Night	Day	Night	Day	Night	Day	Night
1	Surface	44.9	17.2 ± 12.7	15.8 ± 11.2	0.3 ± 0.7	0.0 ± 0.2	79.5 ± 10.6	72.4 ± 4.6	16.9 ± 28.1	6.0 ± 6.2
2	DBDD	28.0	27.3 ± 24.1	19.2 ± 13.7	4.4 ± 3.0	0.0 ± 0.1	113.9 ± 32.4	69.3 ± 4.4	26.8 ± 55.3	4.6 ± 4.2
3	DBDD	2.8	39.5 ± 32.4	28.4 ± 27.5	1.3 ± 0.6	0.1 ± 0.5	126.4 ± 52.1	100.8 ± 23	358.7 ± 206.8	30.3 ± 35.1
4	DBDD	7.3	31.6 ± 27.0	32.0 ± 26.5	2.4 ± 3.1	1.4 ± 0.8	115.1 ± 36.5	103.1 ± 27.0	29.3 ± 58.4	54.8 ± 78.5
5	CDS	15.1	58.7 ± 24.3	54.0 ± 19.8	0.1 ± 0.5	0.0 ± 0.0	144.3 ± 23.2	0.0 ± 0.0	55.6 ± 33.3	0.0 ± 0.0
6	Other	1.8	32.7 ± 37.1	33.2 ± 37.5	5.6 ± 6.9	8.1 ± 3.3	99.7 ± 31.5	110.9 ± 35.4	45.6 ± 131.4	16.3 ± 34.2
7	Other	0.2	23.0 ± 11.7	20.8 ± 8.4	0.3 ± 0.6	1.0	69.4	70.5 ± 4.3	4.0	1054.0 ± 309.2

The mean swimming depths during the daytime and nighttime in this cluster were 58.7 ± 24.3 and 54.0 ± 19.8 m, respectively (Table 2). Cluster 5 noticeably differed from the other clusters because the fish did not enter the surface layer during the daytime or nighttime (Fig. 5E,L). We referred to Cluster 5 as the 'continuous deep swimming' (CDS) mode. The total frequency of Clusters 6 and 7 was less than 2% (Table 2). Although rare behavior might be ecologically important, we assigned these 2 clusters to 'other' behavior for the purposes of this study.

The vertical movement patterns of yellowtails also changed according to the spatiotemporal change in vertical temperature structures (Figs. 6 & 7). The monthly mean daytime depth ranged from 15.4 ± 15.6 m (in July) to 55.1 ± 30.5 m (in December), and was deeper than the depths recorded at night (10.8 ± 15.8 m in June and 48.9 ± 26.0 m in December) for all tagged fish. Thus, yellowtails made diel vertical movements. A seasonal thermocline developed in shallow waters during July and August when tagged fish distributed along the west coast of the Tsugaru Strait to the west coast of Hokkaido (Fig. 7B,C). Mean ILDs of 16.1 ± 2.6 m in July and 18.1 ± 3.2 m in August were recorded for all individuals. The swimming depths of the fish tended to be confined to the shallow mixed layer, with the mean swimming depths of all tagged yellowtails being 13.8 ± 13.9 m in July and 17.5 ± 12.0 m in August. Mean monthly ambient temperature was 20.1 ± 1.8°C in July and 21.9 ± 1.7°C in August for all tagged fish. The surface mode (i.e. when fish mainly swam in the surface layer) was the most frequently documented vertical behavioral mode (62.1%) during the daytime, followed by DBDD through the thermocline (36.1%) (Fig. 8B,C) from July to August. These results showed that yellowtails spent most of their time in the surface mixed layer during the day and night, but sometimes made frequent short dives through the thermocline, especially during the day, in this period. In comparison, CDS was not documented between June and August, because of the shallow thermocline.

Although the seasonal thermocline gradient was still present, ILD gradually increased (Fig. 7D,E) when all tagged fish remained in the waters west of Hokkaido. The mean ILD was 16.2 ± 2.6 m (B2883) and 18.7 ± 3.2 m (B2821) in August, increasing to 35.3 ± 4.5 m (B2826) and 42.1 ± 4.17 m (B2883) in September, and 47.7 ± 14.2 m (B2820) and 59.0 ± 7.6 m (B2883) in October. The thermocline became deeper after August, with fish also swimming in deeper layers in September and October compared to August (Fig. 7D,E). Thus, the range of swimming layer increased with increasing thermocline depth (i.e. ILD). In September and October, the DBDD state was dominant (51.3%), followed by surface (44.2%) (Fig. 8D,E); thus, DBDD below the thermocline occurred frequently in these months. Mean monthly ambient temperature was 21.0 ± 1.5°C (in September for A1393) and 17.0 ± 2.1°C (in October for A1393).

From late October to December, yellowtails migrated southward without entering the offshore coldwater mass, which was corroborated by the ambient temperature experienced by individuals. For example, the ambient temperature (mean: 17.2 ± 0.5 to 18.6 ± 0.4°C) changed minimally in association with vertical movements, and mean ILD ranged from 107.6 ± 11.5 m (B2883) to 123.2 ± 5.4 m (B2824) in December (Fig. 7G), suggesting that yellowtails occupied areas with a temperature structure different from that of the coldwater mass. In addition, individuals rarely swam near the surface, with their swimming depth increasing during the southward movement (Fig. 7F,G). The overall monthly frequency in CDS obtained from all individuals that constantly swam in the deep layer was 61.3% in November and 74.3% in December (Fig. 8F,G). CDS was the most frequently recorded behavior during this period. The

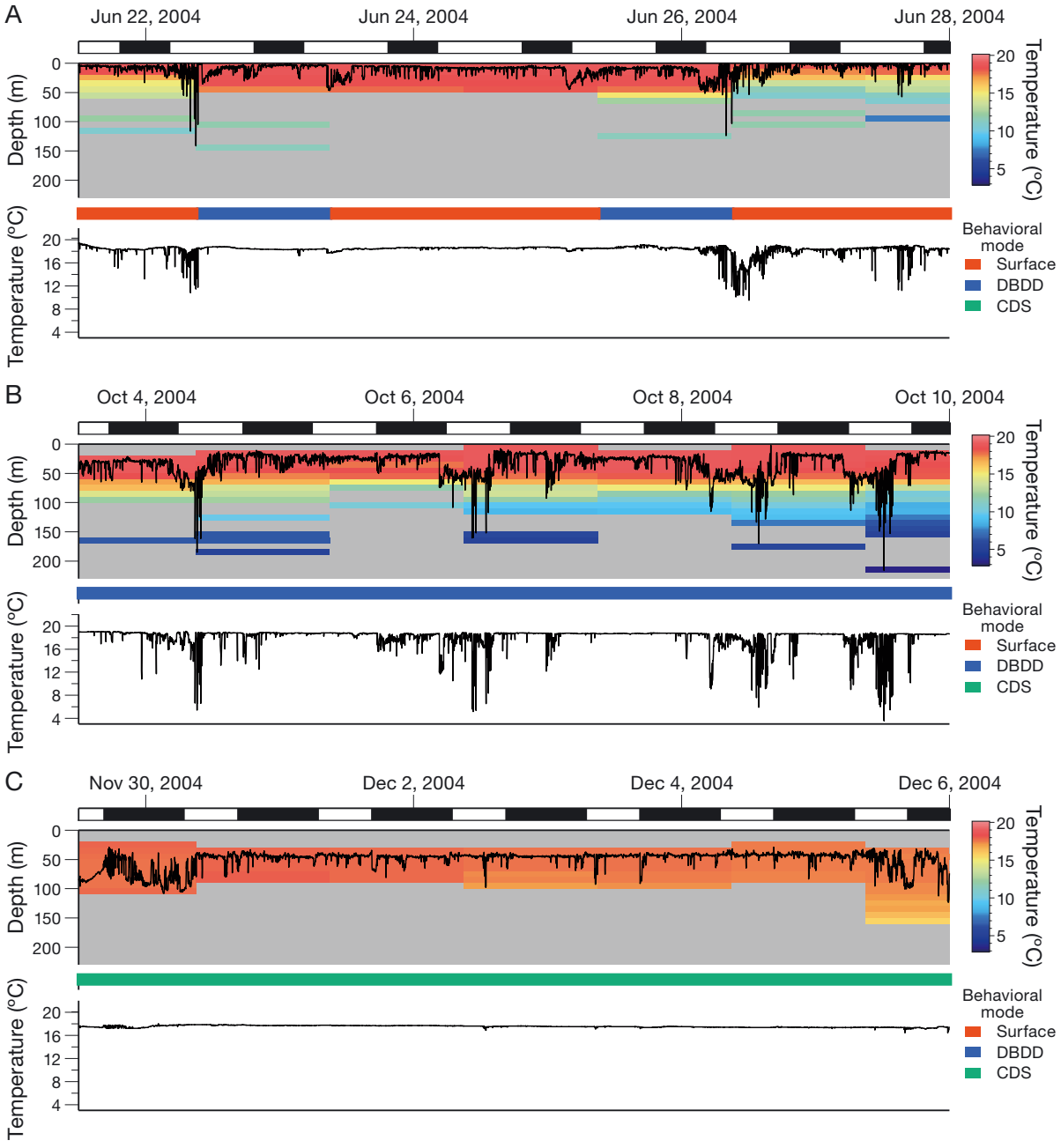

Fig. 6. Weekly time series data in (A) June, (B) October, and (C) November 2004 for swimming depth and vertical thermal structure, behavioral mode (center horizontal bar), and ambient temperature obtained from an individual yellowtail *Seriola quinqueradiata* (tag number B2827). Horizontal black bars indicate nighttime. Behavioral modes were classified based on Greenwich Mean Time at a daily scale (CDS: continuous deep swimming; DBDD: diel brief deep dive)

mean monthly swimming depth was 63.5 ± 21.1 m (in November for B2824) and 34.2 ± 19.8 m (in December for B2827) during this period.

3.3. Effect of environmental factors

The GAMMs identified the thermal environment that was correlated with the habitat use of tagged individuals at the foraging grounds. The best-fitting model included region (longitude and latitude), SST, and interaction of SST and ILD (N = 14 084, residual degrees of freedom = 14 023.95, deviance explained = 76.8%). The smooth terms of all environmental variables included in this model were used as common values for all individuals (Fig. 9). SST smooth term curves showed that the probability of yellowtail occurrence was greater at approximately 18°C (Fig. 9C).

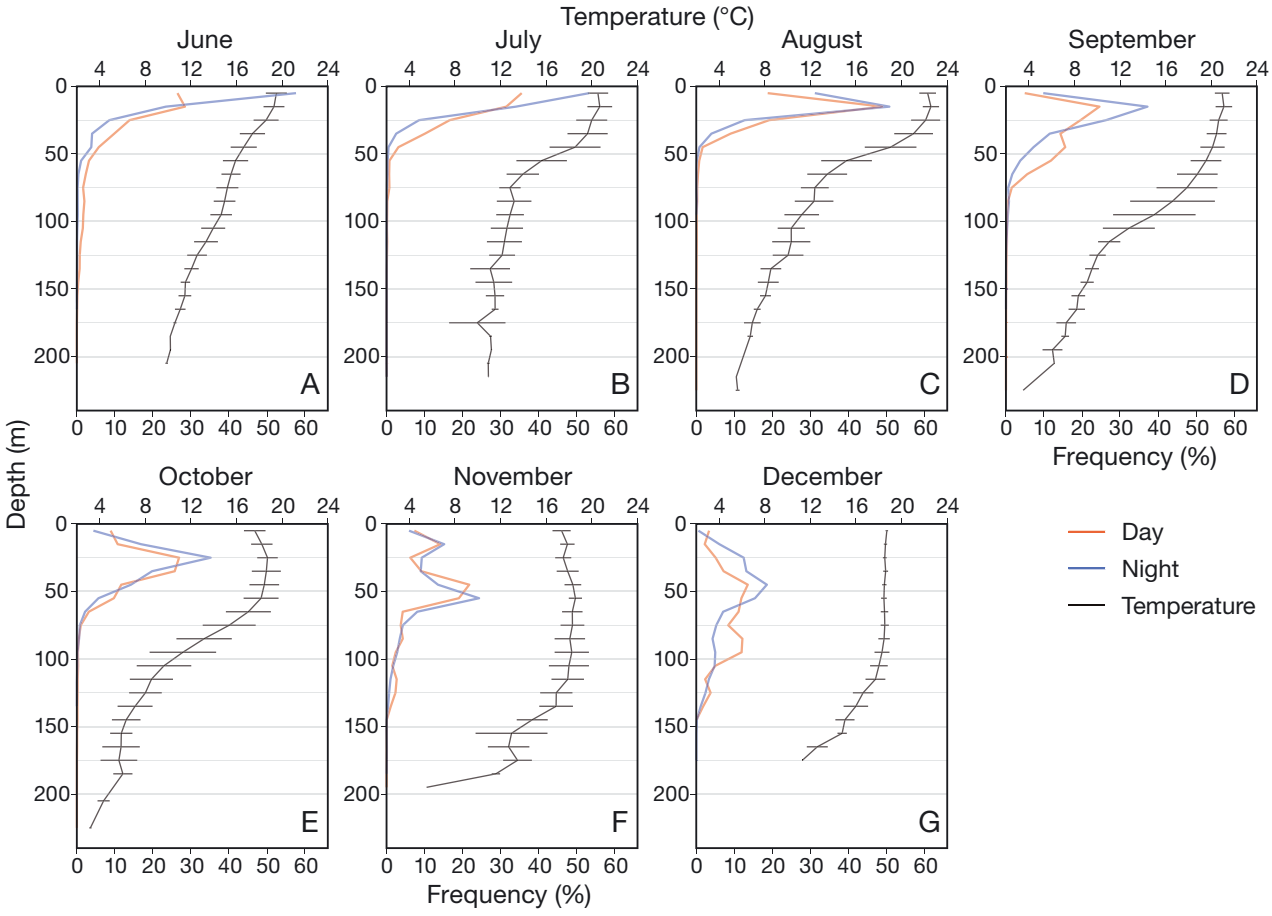

Fig. 7. (A–G) Monthly change in the frequency distribution of the swimming depth of an individual yellowtail *Seriola quinqueradiata* (tag number B2826) during the daytime (red) and nighttime (blue) with the vertical profile of mean ambient water temperature (grey) and standard deviation in each bin

In addition, the interaction of SST and ILD influenced habitat use, even though the ILD-only term was not included in the best-fit model (Fig. 9B). For example, in the low SST area (<18°C), the occurrence of yellowtails was lower in shallow ILD (Fig. 9B), showing that these fish were rarely distributed in the waters where the swimming layer was limited to the surface layer by a shallow thermocline where the water was already cool. However, even if the SST where fish were likely to occur was high (14–24°C), the decrease in occurrence in offshore waters was reflected by the latitude and longitude term (Fig. 9A) because the fish were moving along the coast.

The MLR model showed that vertical movement patterns were affected by ILD (i.e. thermocline, Fig. 10; N = 1527, residual degrees of freedom = 1509.318, deviance explained = 28.8%). Furthermore, SST and regional effect (longitude and latitude) were not included in the best-fit model. Surface behavior was frequent when ILD was shallow; however, as ILD became deeper, intermittent deep dives across the thermocline during the daytime (DBDD mode) increased. Yet, DBDD did not monotonically increase with increasing ILD, and the percentage of DBDD peaked when ILD was 40.5 to 61.5 m, ranging from 26.8 to 63.5%. This condition was established in the area to the west of Hokkaido in September and October (Fig. 8D,E, K,L). As the ILD deepened (>80 m, approximately), CDS was predominant for all individuals (Figs. 8F,G & 10). This phenomenon corresponded to the period when yellowtails were migrating along the coast of Honshu in November and December (Fig. 8F,G,M,N).

4. DISCUSSION

By applying the state-space model to the geolocation data of yellowtails obtained in the Japan Sea, the relationship between individual behaviors and oce-

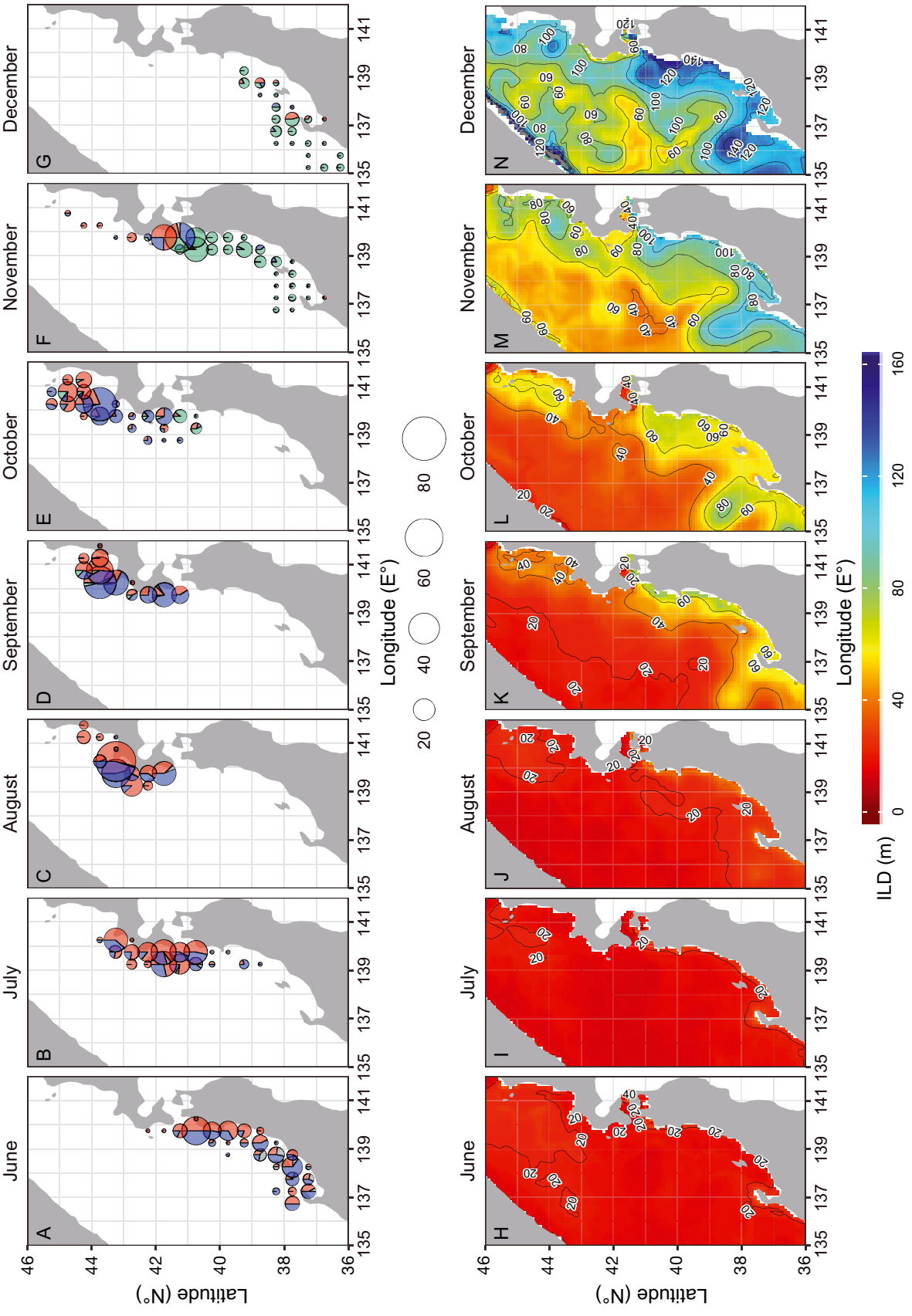

Fig. 8. (A–G) Monthly change in pooled individual yellowtail *Seriola quinqueradiata* distribution and fraction of the behavioral mode classified as surface (orange), diel brief deep dive (blue), continuous deep swimming (green), and other (grey). Circle size indicates the cumulative total number of observed days in each 0.5° × 0.5° grid cell. (H–N) Monthly change in horizontal distribution of the isothermal layer depth (ILD)

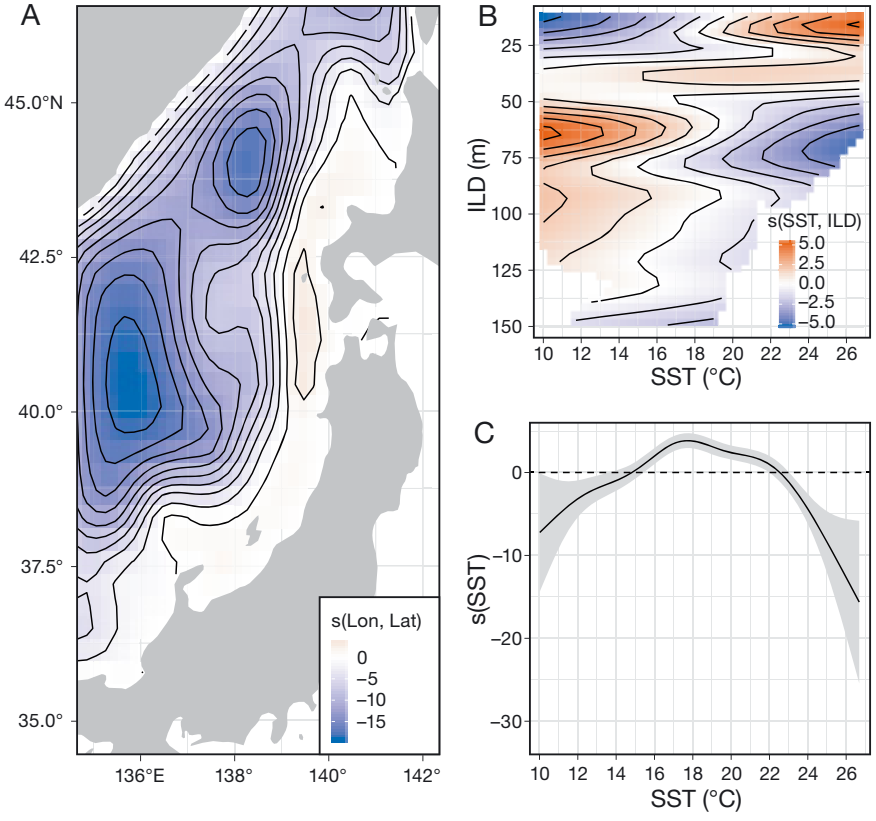

Fig. 9. Estimated response curves (smooth terms) from the best-fit generalized additive mixed model. (A) Longitude and latitude, (B) interaction of sea surface temperature (SST) and isothermal layer depth (ILD), and (C) SST. Grey area in (C) represents the 95% confidence intervals

anic temperature structures was examined at an unprecedented level. The state-space model represents a significant improvement in removing noisy data from non-likelihood-based methods (Sibert et al. 2003, Jonsen et al. 2005). However, state-space approaches were not used to improve geolocation data in a previous archival tagging study for yellowtails (Ino et al. 2008), which was only able to report rough estimates of the average location of individuals at one point per month. Therefore, that study did not report a yellowtail migratory response to the spatio-temporal change in water temperature structure in the Japan Sea.

In our study, the horizontal movement of tagged yellowtails along the northwestern Japanese coast in the northeastern Japan Sea was roughly divided into 3 phases: (1) northward movement from June to July, (2) residency in the northern area from August to late October, and (3) southward movement from November to December. These observations reflect the general spatio-temporal changes in set net fishing conditions for large-sized yellowtails in the Japan Sea (Mitani 1960). Because yellowtails spent most of their time within the surface mixed layer above the thermocline, SST represents a good indicator of movement and distribution. In fact, significantly more yellowtails were present when SST ranged approximately from 16 to 21°C (Fig. 9C). This observation was similar to that obtained by a previous archival tagging study around the Noto Peninsula to the west of Hokkaido in the same season (Ino et al. 2008). However, even though the range over which the smooth term of SST was high (approximately 16–21°C, Fig. 9C), yellowtails did not use offshore areas but were instead distributed along the coast. The water mass structure, such as the location and movement of cold-water eddies, affects the yellowtail fishery conditions (Ogawa 1976, Hara 1990). None of the 8 fish analyzed in the current study entered the coldwater mass that formed offshore. Consequently, it was not possible to distinguish whether the yellowtails were absent in the offshore because of the regional effect or the structure of the water temperature. The thermal structure of the Japan Sea changes across years (Isoda 1994, Choi et al. 2009, You et al. 2010, Zhao et al. 2014). Accumulation of multi-year archival tag data could reveal the relationship between annual variations in water temperature structure and yellowtail movements, although our present study only included a single year of data, and only 8 fish.

The vertical movement pattern of yellowtails also changed seasonally and was influenced by spatio-temporal changes in the temperature structure. The tagged fish were mainly distributed within the surface mixed layer (Fig. 7); thus, yellowtails might have avoided entering colder water beyond the thermocline. However, while yellowtails predominantly occupied the mixed layer (surface mode), they made frequent short dives through the thermocline (DDBD), especially during the daytime. A similar phenomenon has been recorded in other fishes (Kitagawa et al. 2000, 2004, Thums et al. 2013, Nakamura et al. 2015, Furukawa et al. 2017), in which frequent dives were associated with foraging. Although yellowtail feeding habits have not been directly observed in our study area, the stomach contents of adult yellowtails

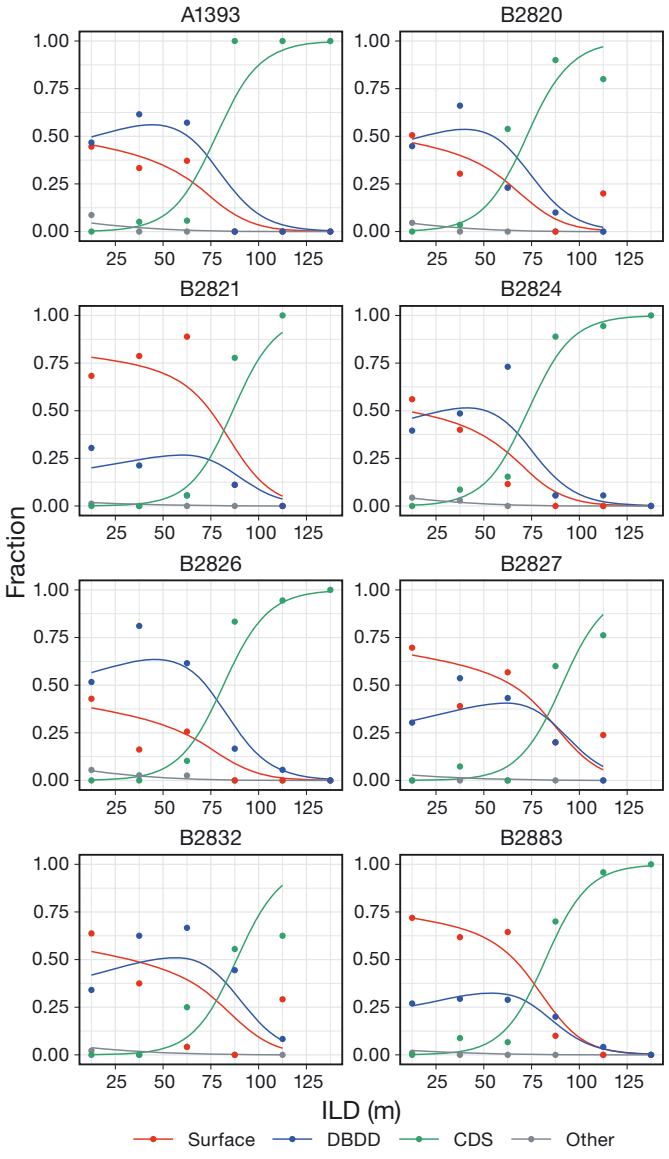

Fig. 10. Relationship between isothermal layer depth (ILD) and the fraction of the behavioral mode for each individual. Regression lines are represented by solid lines and circles represent the fraction of behavioral mode for each 25 m bin (CDS: continuous deep swimming; DBDD: diel brief deep dive)

caught in Wakasa Bay in the Japan Sea have been reported (Mitani 1960). This previous study revealed that yellowtails are opportunistic feeders that consume a variety of prey species, including *Trachurus japonicus*, *Engraulis japonicus*, *E. teres*, *Sardinops melanostictus*, *Scomber japonicus*, and *Todarodes pacificus*. Of these, *E. japonicus*, *S. melanostictus*, and *E. teres* are distributed in the upper layers of the thermocline (Ohshimo 2004, Charef et al. 2010). However, some of the main prey species of yellowtails are typically distributed below the thermocline, including *T. japonicus* (Nakamura & Hamano 2009) and *T. pacificus* (Suzuki et al. 1974, Fujino et al. 2010), suggesting that frequent dives below the thermocline may be related to foraging.

The fraction of the vertical behavioral mode (surface, DBDD, and CDS) changed with increasing ILD (Fig. 10). When a thermocline developed at a shallow depth, the surface mode was the primary behavior during the northward movement period from June to July and during residency to the west of Hokkaido in August, with DBDD also being observed. Thus, yellowtails might preferentially forage near the surface over diving to deeper waters when thermoclines develop in shallow waters. Thermal stratification at the depth of the thermocline provides a physical means of vertically aggregating prey species (Hansen et al. 2001, Gray & Kingsford 2003, Pelletier et al. 2012). Thus, yellowtails might maximize the probability of encountering prey through horizontal movements near the surface when thermoclines develop in shallow water.

From September to October, tagged fish remained to the west of Hokkaido, with DBDD representing the most frequent behavioral mode, while the ILD became deeper compared to August. A deeper thermocline might reduce encounters with prey organisms on the surface, which might increase the number of dives made by yellowtails beneath the thermocline. Of note, more fishing activity for the Japanese flying squid *T. pacificus* typically occurs in this region than in any other region of the northeastern Japan Sea coast from September to October (Kidokoro 2009, Alabia et al. 2016), with *T. pacificus* being distributed below the thermocline during the daytime in this region (Suzuki et al. 1974, Fujino et al. 2010). *T. pacificus* is a large-scale fishery resource in the Japan Sea (Arkhipkin et al. 2015, Kubota et al. 2019b) and plays critical roles in marine food webs by serving as an important prey species for numerous marine predators (Ohizumi et al. 2000), including yellowtails (Sakurai et al. 2013). Consequently, there is a high biomass of potential prey species, such as flying squid, below the thermocline in this area. In addition, all individuals exhibited resident or slow movement states in areas west of Hokkaido during the summer to autumn months, which are not associated with spawning (Kubota et al. 2019a), although the vertical swimming pattern was not dependent on the horizontal movement state based on our statistical analysis. The prey biomass and individual residence state phenomena suggest that the area west of Hokkaido plays an important role as a feeding ground for yellowtails in the Japan Sea.

From November to December, yellowtails rapidly migrated southward in CDS mode, which was not ob-

served in any other period. In particular, Mitani (1960) reported that many large yellowtails caught during the southward movement had empty stomachs, which might reflect a period of reduced feeding frequency associated with spawning. Therefore, this vertical movement pattern was probably not related to foraging. There is a northeastward current derived from the Tsushima Warm Current along the southward movement path of yellowtails that has a generally strong current velocity at the surface (Watanabe et al. 2006). Because the vertical temperature was homogeneous during this period, yellowtails consistently swam in the deep-water layers. Swimming in deep water might help conserve energy during the southward movement.

In this study, we demonstrated that horizontal and vertical movement of yellowtails is driven by oceanographic thermal conditions. We believe that this new information helps to understand the external factors affecting their movements, which is essential for establishing a movement ecology paradigm (Nathan et al. 2008). However, the sample size and fish size classes were limited. Consequently, we did not obtain the movement pattern of individuals moving from the Japan Sea to the East China Sea, or of individuals that remained year-round in the middle part of the Japan sea coast, as previously reported (Ino et al. 2008). The geolocation data analysis used in this study for individuals showing these movement patterns will clarify the fishing processes associated with these migratory routes, which were not revealed by previous rough location estimates of Ino et al. (2008). In addition, since sexing of the tagged fish was not performed in this study, it was not possible to examine sex-specific differences in behavior. As some migratory fish show different migratory habits between males and females (Shimose et al. 2012), it will be necessary to consider the sex of individuals in future studies. Furthermore, movement patterns might differ for each age (or size) class (Maeda et al. 2010). In addition to further archival tagging surveys, re-analysis of the past dataset (e.g. Ino et al. 2008) using modern analysis techniques, such as the state-space model, are needed to elucidate population level movement patterns of yellowtails.

Acknowledgements. We sincerely thank the members of Ohsawa set net fishers association for supporting the field research. We also thank everyone who assisted with tag recovery. Y. Sogawa helped with organizing the archival tag data. This study used the dataset 'Four-dimensional Variational Ocean Reanalysis for the western North Pacific' (FORA-WNP30), which was produced by the Japan Agency for Marine-Science and Technology (JAMSTEC) and the Meteorological Research Institute of the Japan Meteorological Agency (JMA/MRI). The research was supported by a grant from the Japan Fisheries Agency and JSPS KAKENHI Grant Number JP18K14518.

LITERATURE CITED

Alabia ID, Dehara M, Saitoh SI, Hirawake T (2016) Seasonal habitat patterns of Japanese common squid (*Todarodes pacificus*) inferred from satellite-based species distribution models. Remote Sens 8:921

Amante C, Eakins BW (2009) ETOPO1 1 Arc-minute global relief model: procedures, data sources and analysis. NOAA Tech Memo NESDIS NGDC-24

Arkhipkin AI, Rodhouse PGK, Pierce GJ, Sauer W and others (2015) World squid fisheries. Rev Fish Sci Aquacult 23:92–252

Block BA, Jonsen ID, Jorgensen SJ, Winship AJ and others (2011) Tracking apex marine predator movements in a dynamic ocean. Nature 475:86–90

Brownscombe JW, Cooke SJ, Algera DA, Hanson KC and others (2017) Ecology of exercise in wild fish: integrating concepts of individual physiological capacity, behavior, and fitness through diverse case studies. Integr Comp Biol 57:281–292

Carvalho F, Ahrens R, Murie D, Bigelow K, Aires-Da-Silva A, Maunder MN, Hazin F (2015) Using pop-up satellite archival tags to inform selectivity in fisheries stock assessment models: a case study for the blue shark in the South Atlantic Ocean. ICES J Mar Sci 72:1715–1730

Charef A, Ohshimo S, Aoki I, Al Absi N (2010) Classification of fish schools based on evaluation of acoustic descriptor characteristics. Fish Sci 76:1–11

Chmura HE, Glass TW, Williams CT (2018) Biologging physiological and ecological responses to climatic variation: new tools for the climate change era. Front Ecol Evol 6:92

Choi BJ, Haidvogel DB, Cho YK (2009) Interannual variation of the Polar Front in the Japan/East Sea from summertime hydrography and sea level data. J Mar Syst 78:351–362

Crawshaw LI (1977) Physiological and behavioral reactions of fishes to temperature change. J Fish Res Board Can 34: 730–734

Davis RW, Fuiman LA, Williams TM, Horning M, Hagey W (2003) Classification of Weddell seal dives based on 3-dimensional movements and video-recorded observations. Mar Ecol Prog Ser 264:109–122

Ekstrom P (2007) Error measures for template-fit geolocation based on light. Deep Sea Res II 54:392–403

Fujino T, Kawabata A, Kidokoro H (2010) Echograms of aquatic organisms observed by a quantitative echosounder around Japan. Japan Sea Fisheries Research Institute, Niigata. http://jsnfri.fra.affrc.go.jp/shigen/echocata

Fujioka K, Fukuda H, Furukawa S, Tei Y, Okamoto S, Ohshimo S (2018) Habitat use and movement patterns of small (age-0) juvenile Pacific bluefin tuna (*Thunnus orientalis*) relative to the Kuroshio. Fish Oceanogr 27:185–198

Furukawa S, Fujioka K, Fukuda H, Suzuki N, Tei Y, Ohshimo S (2017) Archival tagging reveals swimming depth and ambient and peritoneal cavity temperature in age-0 Pacific bluefin tuna, *Thunnus orientalis*, off the southern coast of Japan. Environ Biol Fishes 100:35–48

Gray CA, Kingsford MJ (2003) Variability in thermocline depth and strength, and relationships with vertical distributions of fish larvae and mesozooplankton in dynamic coastal waters. Mar Ecol Prog Ser 247:211–224

Gunn J, Polacheck T, Davis T, Sherlock M, Betlehem A (1994) The development and use of archival tags for studying the migration, behaviour and physiology of southern bluefin tuna, with an assessment of the potential for transfer of the technology to groundfish research. ICES Mini Symposium on Fish Migration, ICES, Copenhagen

Hansen JE, Martos P, Madirolas A (2001) Relationship between spatial distribution of the Patagonian stock of Argentine anchovy, *Engraulis anchoita*, and sea temperatures during late spring to early summer. Fish Oceanogr 10:193–206

Hara N (1990) Yearly fluctuations of yellowtail catch in set net fishery along the coastal area of the Sea of Japan. Bull Jpn Soc Sci Fish 56:25–30

Hasegawa T, Takatsuki N, Kawabata Y, Kawabe R and others (2017) Continuous behavioral observation reveals the function of drifting seaweeds for *Seriola* spp. juveniles. Mar Ecol Prog Ser 573:101–115

Hays GC, Ferreira LC, Sequeira AMM, Meekan MG and others (2016) Key questions in marine megafauna movement ecology. Trends Ecol Evol 31:463–475

Ino S, Nitta A, Kohno N, Tsuji T, Okuno J, Yamamoto T (2008) Migration of the adult yellowtail (*Seriola quinqueradiata*) as estimated by archival tagging experiments in the Tsushima Warm Current. Bull Jpn Soc Fish Oceanogr 72:92–100

Isoda Y (1994) Warm eddy movements in the eastern Japan/East Sea. J Oceanogr 50:1–15

Jonsen I (2016) Joint estimation over multiple individuals improves behavioural state inference from animal movement data. Sci Rep 6:20625

Jonsen ID, Flemming JM, Myers RA (2005) Robust state-space modeling of animal movement data. Ecology 86: 2874–2880

Jonsen ID, Basson M, Bestley S, Bravington MV and others (2013) State-space models for bio-loggers: a methodological road map. Deep Sea Res II 88-89:34–46

Kara AB, Rochford PA, Hurlburt HE (2000) An optimal definition for ocean mixed layer depth. J Geophys Res 105: 16803–16821

Kasai A, Sakamoto W, Mitsunaga Y, Yamamoto S (2000) Behaviour of immature yellowtails (*Seriola quinqueradiata*) observed by electronic data-recording tags. Fish Oceanogr 9:259–270

Kidokoro H (2009) Changes in the landing of common squid *Todarodes pacificus* in the coastal areas of the Sea of Japan during 1994-2007. Rep 2008 Annu Meet Squid Resour, p 48–57 (in Japanese)

Kitagawa T, Nakata H, Kimura S, Itoh T, Tsuji S, Nitta A (2000) Effect of ambient temperature on the vertical distribution and movement of Pacific bluefin tuna *Thunnus thynnus orientalis.* Mar Ecol Prog Ser 206:251–260

Kitagawa T, Kimura S, Nakata H, Yamada H (2004) Diving behavior of immature, feeding Pacific bluefin tuna (*Thunnus thynnus orientalis*) in relation to season and area: the East China Sea and the Kuroshio-Oyashio transition region. Fish Oceanogr 13:161–180

Kitagawa T, Boustany AM, Farwell CJ, Williams TD, Castleton MR, Block BA (2007) Horizontal and vertical movements of juvenile bluefin tuna (*Thunnus orientalis*) in relation to seasons and oceanographic conditions in the eastern Pacific Ocean. Fish Oceanogr 16:409–421

Kubota H, Furukawa S, Matsukura R, Watari S (2019a) Stock assessment and evaluation for yellowtail (fiscal year 2018). In: Marine fisheries stock assessment and evaluation for Japanese waters (fiscal year 2018/2019). Fisheries Agency and Fisheries Research and Education Agency of Japan, p 1364–1401 (in Japanese)

Kubota H, Miyahara H, Matsukura R (2019b) Stock assessment and evaluation for autumn spawning stock of Japanese flying squid (fiscal year 2018). In: Marine fisheries stock assessment and evaluation for Japanese waters (fiscal year 2018/2019). Fisheries Agency and Fisheries Research and Education Agency of Japan, p 698–745 (in Japanese)

Lam CH, Nielsen A, Sibert JR (2008) Improving light and temperature based geolocation by unscented Kalman filtering. Fish Res 91:15–25

Lam CH, Nielsen A, Sibert JR (2010) Incorporating sea-surface temperature to the light-based geolocation model TrackIt. Mar Ecol Prog Ser 419:71–84

Lesage V, Hammill MO, Kovacs KM (1999) Functional classification of harbor seal (*Phoca vitulina*) dives using depth profiles, swimming velocity, and an index of foraging success. Can J Zool 77:74–87

Lowerre-Barbieri SK, Kays R, Thorson JT, Wikelski M (2019) The ocean's movescape: fisheries management in the bio-logging decade (2018–2028). ICES J Mar Sci 76: 477–488

Lunn DJ, Thomas A, Best N, Spiegelhalter D (2000) WinBUGS — a Bayesian modelling framework: concepts, structure, and extensibility. Stat Comput 10:325–337

Maeda H, Watanabe K, Ino S, Okuno J (2010) On migration group by the age. In: Kishida T (ed) Elucidation of the relationship between migration pattern and sea environment, and prediction method of relative abundance for yellowtail in the Japanese waters. Bull Fish Res Agen Yokohama 30:5–10 (in Japanese with English abstract)

Magnuson JJ, Crowder LB, Medvick PA (1979) Temperature as an ecological resource. Am Zool 19:331–343

McGowan J, Beger M, Lewison RL, Harcourt R and others (2017) Integrating research using animal-borne telemetry with the needs of conservation management. J Appl Ecol 54:423–429

Mitani F (1960) Fishery biology of the yellow-tail, *Seriola quinqueradiata* T. & S., inhabiting the waters around Japan. Mem Fac Agric Kinki Univ 1:81–300 (in Japanese with English abstract)

Murayama T (1992) Fisheries biology of yellowtail in the Japan Sea. Rep Shimane Pref Fish Exp Stn 7:1–64 (in Japanese with English abstract)

Musyl M, Brill R, Curran D, Gunn JS and others (2001) Ability of archival tags to provide estimates of geographical position based on light intensity. In: Sibert JR, Nielsen JL (eds) Electronic tagging and tracking in marine fisheries. Kluwer, Dordrecht, p 343–368

Nakamura T, Hamano A (2009) Seasonal differences in the vertical distribution pattern of Japanese jack mackerel, *Trachurus japonicus*: changes according to age? ICES J Mar Sci 66:1289–1295

Nakamura I, Goto Y, Sato K (2015) Ocean sunfish rewarm at the surface after deep excursions to forage for siphonophores. J Anim Ecol 84:590–603

Nathan R, Getz WM, Revilla E, Holyoak M, Kadmon R, Saltz D, Smouse PE (2008) A movement ecology paradigm for unifying organismal movement research. Proc Natl Acad Sci USA 105:19052–19059

Nielsen A, Bigelow KA, Musyl MK, Sibert JR (2006) Improving light-based geolocation by including sea surface temperature. Fish Oceanogr 15:314–325

Ochiai A, Tanaka M (1986) Yellowtail. In: Ochiai A, Tanaka M (eds) Ichthyology. Koseisha-Koseikaku, Tokyo, p 788–797 (in Japanese)

Ogawa Y (1976) Interrelationship between changes of location of a cold-water mass off Shimane and fishing condition of yellowtail shore-net. Bull Jpn Soc Sci Fish Oceanogr 29:1–6 (in Japanese with English abstract)

Ohizumi H, Kuramochi T, Amano M, Miyazaki N (2000) Prey switching of Dall's porpoise *Phocoenoides dalli* with population decline of Japanese pilchard *Sardinops melanostictus* around Hokkaido, Japan. Mar Ecol Prog Ser 200:265–275

Ohno M (1984) Algological observation on the floating seaweeds of offshore water of Shikoku Island in Japan. Bull Jpn Soc Sci Fish 50:1653–1656 (in Japanese with English abstract)

Ohshimo S (2004) Spatial distribution and biomass of pelagic fish in the East China Sea in summer, based on acoustic surveys from 1997 to 2001. Fish Sci 70:389–400

Pante E, Simon-Bouhet B (2013) Marmap: a package for importing, plotting and analyzing bathymetric and topographic data in R. PLOS ONE 8:e73051

Pelletier L, Kato A, Chiaradia A, Ropert-Coudert Y (2012) Can thermoclines be a cue to prey distribution for marine top predators? A case study with little penguins. PLOS ONE7:e31768

Plummer M (2016) rjags: Bayesian graphical models using MCMC. R package version 4-6. https://CRAN.R-project.org/package=rjags

Plummer M (2017) JAGS: just another Gibbs sampler. Version 4.3.0. http://mcmc-jags.sourceforge.net

R Core Team (2019) R: a language and environment for statistical computing. R Foundation for Statistical Computing, Vienna

Sakamoto KQ, Sato K, Ishizuka M, Watanuki Y, Takahashi A, Daunt F, Wanless S (2009) Can ethograms be automatically generated using body acceleration data from free-ranging birds? PLOS ONE 4:e5379

Sakurai Y, Kidokoro H, Yamashita N, Yamamoto J, Uchikawa K, Takahara H (2013) *Todarodes pacificus*, Japanese common squid. In: Rosa R, O'Dor R, Pierce GJ (eds) Advances in squid biology, ecology and fisheries. Part II — Oegopsid squids. Nova Science Publishers, New York, NY, p 249–271

Schreer JF, Testa JW (1996) Classification of Weddell seal diving behavior. Mar Mamm Sci 12:227–250

Secor DH (2015) Migration ecology of marine fishes. Johns Hopkins University Press, Baltimore, MD

Shimose T, Yokawa K, Saito H, Tachihara K (2012) Sexual difference in the migration pattern of blue marlin, *Makaira nigricans*, related to spawning and feeding activities in the western and central North Pacific Ocean. Bull Mar Sci 88:231–250

Shiraishi T, Ohshima S, Yukami R (2011) Age, growth and reproductive characteristics of yellowtail (*Seriola quinqueradiata*) caught in the waters off western Kyushu. Bull Jpn Soc Fish Oceanogr 75:1–8 (in Japanese with English abstract)

Sibert JR, Musyl MK, Brill RW (2003) Horizontal movements of bigeye tuna (*Thunnus obesus*) near Hawaii determined by Kalman filter analysis of archival tagging data. Fish Oceanogr 12:141–151

Sippel T, Eveson JP, Galuardi B, Lam C and others (2015) Using movement data from electronic tags in fisheries stock assessment: a review of models, technology and experimental design. Fish Res 163:152–160

Suzuki T, Tashiro M, Yamagishi Y (1974) Studies on the swimming layer of squid *Todarodes pacificus* (Steenstrup) as observed by a fish finder in the offshore region of the northern part of the Japan Sea. Bull Fac Fish Hokkaido Univ 25:238–246 (in Japanese with English abstract)

Tanaka S (1984) Migration model and dynamics parameters of large-sized yellowtails in the Pacific along the Japanese coast inferred from tag recaptures after the year of release. Nippon Suisan Gakkaishi 50:1341–1347

Taylor NG, McAllister MK, Lawson GL, Carruthers T, Block BA (2011) Atlantic bluefin tuna: a novel multistock spatial model for assessing population biomass. PLOS ONE 6:e27693

Teo SLH, Boustany A, Blackwell S, Walli A, Weng KC, Block BA (2004) Validation of geolocation estimates based on light level and sea surface temperature from electronic tags. Mar Ecol Prog Ser 283:81–98

Thums M, Meekan M, Stevens J, Wilson S, Polovina J (2013) Evidence for behavioural thermoregulation by the world's largest fish. J R Soc Interface 10:20120477

Tian Y, Kidokoro H, Watanabe T, Igeta Y, Sakaji H, Ino S (2012) Response of yellowtail, *Seriola quinqueradiata*, a key large predatory fish in the Japan Sea, to sea water temperature over the last century and potential effects of global warming. J Mar Syst 91:1–10

Tibshirani R, Walther G, Hastie T (2001) Estimating the number of clusters in a data set via the gap statistic. J R Stat Soc Ser B Stat Methodol 63:411–423

Uehara S, Taggart CT, Mitani T, Suthers IM (2006) The abundance of juvenile yellowtail (*Seriola quinqueradiata*) near the Kuroshio: the roles of drifting seaweed and regional hydrography. Fish Oceanogr 15:351–362

Usui N, Wakamatsu T, Tanaka Y, Hirose N and others (2017) Four-dimensional variational ocean reanalysis: a 30-year high-resolution dataset in the western North Pacific (FORA-WNP30). J Oceanogr 73:205–233

Watanabe T, Katoh O, Yamada H (2006) Structure of the Tsushima warm current in the northeastern Japan Sea. J Oceanogr 62:527–538

Wood SN (2008) Fast stable direct fitting and smoothness selection for generalized additive models. J R Stat Soc Ser B Stat Methodol 70:495–518

Wood SN, Bravington MV, Hedley SL (2008) Soap film smoothing. J R Stat Soc Ser B Stat Methodol 70: 931–955

Yamamoto T, Ino S, Kuno M, Sakaji H, Hiyama Y, Kishida T, Ishida Y (2007) On the spawning and migration of yellowtail *Seriola quinqueradiata* and research required to allow catch forecasting. Bull Fish Res Agency Jpn 21: 1–29 (in Japanese)

Yasuda T, Katsumata H, Kawabe R, Nakatsuka N, Kurita Y (2013) Identifying spawning events in the Japanese flounder *Paralichthys olivaceus* from depth time-series data. J Sea Res 75:33–40

You Y, Chang KI, Yun JY, Kim KR (2010) Thermocline circulation and ventilation of the East/Japan Sea, part I: water-mass characteristics and transports. Deep Sea Res II 57:1221–1246

Zhao N, Manda A, Han Z (2014) Frontogenesis and frontolysis of the subpolar front in the surface mixed layer of the Japan Sea. J Geophys Res Oceans 119:1498–1509

Editorial responsibility: Elliott Hazen, Pacific Grove, California, USA

Submitted: May 14, 2019; Accepted: December 19, 2019
Proofs received from author(s): February 14, 2020